

This article was downloaded by:

On: 23 January 2011

Access details: *Access Details: Free Access*

Publisher *Taylor & Francis*

Informa Ltd Registered in England and Wales Registered Number: 1072954 Registered office: Mortimer House, 37-41 Mortimer Street, London W1T 3JH, UK



Journal of Coordination Chemistry

Publication details, including instructions for authors and subscription information:

<http://www.informaworld.com/smpp/title~content=t713455674>

Mono- and di-nuclear azido η^6 -*p*-cymene ruthenium(II) complexes; synthesis, reactivity, and structures

R. Lalrempuia^a; Hemant P. Yennawar^b; Mohan Rao Kollipara^a

^a Department of Chemistry, School of Physical Sciences, North-Eastern Hill University, Shillong, India

^b Department of Biochemistry and Molecular Biology, 8A Althouse Laboratory, The Pennsylvania State University, University Park, PA 16802, USA

First published on: 10 December 2009

To cite this Article Lalrempuia, R. , Yennawar, Hemant P. and Kollipara, Mohan Rao(2009) 'Mono- and di-nuclear azido η^6 -*p*-cymene ruthenium(II) complexes; synthesis, reactivity, and structures', *Journal of Coordination Chemistry*, 62: 22, 3661 – 3678, First published on: 10 December 2009 (iFirst)

To link to this Article: DOI: 10.1080/00958970903154470

URL: <http://dx.doi.org/10.1080/00958970903154470>

PLEASE SCROLL DOWN FOR ARTICLE

Full terms and conditions of use: <http://www.informaworld.com/terms-and-conditions-of-access.pdf>

This article may be used for research, teaching and private study purposes. Any substantial or systematic reproduction, re-distribution, re-selling, loan or sub-licensing, systematic supply or distribution in any form to anyone is expressly forbidden.

The publisher does not give any warranty express or implied or make any representation that the contents will be complete or accurate or up to date. The accuracy of any instructions, formulae and drug doses should be independently verified with primary sources. The publisher shall not be liable for any loss, actions, claims, proceedings, demand or costs or damages whatsoever or howsoever caused arising directly or indirectly in connection with or arising out of the use of this material.

Mono- and di-nuclear azido η^6 -*p*-cymene ruthenium(II) complexes; synthesis, reactivity, and structures

R. LALREMPUIA*[†], HEMANT P. YENNAWAR[‡] and
MOHAN RAO KOLLIPARA*[†]

[†]Department of Chemistry, School of Physical Sciences, North-Eastern Hill University,
Shillong, 793022, India

[‡]Department of Biochemistry and Molecular Biology, 8A Althouse Laboratory,
The Pennsylvania State University, University Park, PA 16802, USA

(Received 26 January 2009; in final form 6 May 2009)

The azide bridge complex $[(\eta^6\text{-}p\text{-cymene})\text{Ru}(\mu\text{-N}_3)\text{Cl}]_2$ (**2**) was prepared from the reaction of sodium azide with $[(\eta^6\text{-}p\text{-cymene})\text{RuCl}]_2$ in ethanol. The molecular structures and spectroscopic properties of the various azido ruthenium complexes so obtained from the reaction with monodentate and bidentate ligands are described.

Keywords: Ruthenium; Arene; Azide; *p*-Cymene

1. Introduction

Arene compounds of ruthenium are a well-established family of robust metal-organic molecules that play an increasingly important role in the organometallic chemistry mainly due to their importance in homogeneous catalysis [1] and their possible contribution as anticancer medicines [2]. For the parent halide bridged compounds $[(\eta^6\text{-arene})\text{RuX}_2]_2$ (arene = *p*-cymene, mesitylene, benzene, hexamethylbenzene, etc.; X = Cl, Br, I) and their numerous derivatives, much information on synthesis and general properties is available [3]. These well-established, halo-bridged compounds in general may be exploited to obtain various ruthenium complexes via cleavage of halide bridges or through the scission of hexa-hapto bound arene [4]. In continuation of our work on synthesis of derivatives of arene ruthenium azido complexes [5], we have reported the synthesis and properties of a wider range of mono- and dinuclear *p*-cymene ruthenium(II) azido complexes prepared directly from **2** as well as some compounds that result from subsequent reactions, and we have also described some contrasting behavior of **2** as compared with the hexamethylbenzene analog. We also describe a small modification of the published synthesis of **2**, which gives consistently high yields. The only *p*-cymene-ruthenium-azido complex reported at present is **2**, obtained

*Corresponding author. Email: lrpa@rediffmail.com; kmrao@nehu.ac.in

from $[(\eta^6\text{-}p\text{-cymene})\text{RuCl}_2]_2$ and trimethylsilyl azide, and no further work was pursued to study its reactivity [6]. This report includes the preparations, properties, and structures of selected compounds of various mono- and di-nuclear azido-ruthenium complexes bearing *p*-cymene, and we have demonstrated here very similar reactivity of $\mu\text{-N}_3$ compared to $\mu\text{-Cl}$, particularly in regards to the cleavage-substitution reaction.

2. Results and discussion

The reaction of $[(\eta^6\text{-}p\text{-cymene})\text{RuCl}_2]_2$ with sodium azide at ambient temperature in ethanol rapidly yielded an air stable, orange crystalline compound which shows very strong IR absorption at 2057 cm^{-1} , assignable to end-on bridging ($\mu\text{-1,1}$) azide [7]. ^1H NMR spectrum clearly indicates the presence of *p*-cymene moiety and this compound appears to be same as the complex obtained from reaction between $[(\eta^6\text{-}p\text{-cymene})\text{RuCl}_2]_2$ and trimethylsilyl azide reported by Bates *et al.* [6]. We have carried out the structural determination and it indeed proved that the compounds are identical having the formula $[(\eta^6\text{-}p\text{-cymene})\text{Ru}(\mu\text{-N}_3)\text{Cl}]_2$ (**2**); however, the structural data of **2** is neither reported nor discussed here as Bates *et al.* have published it earlier.

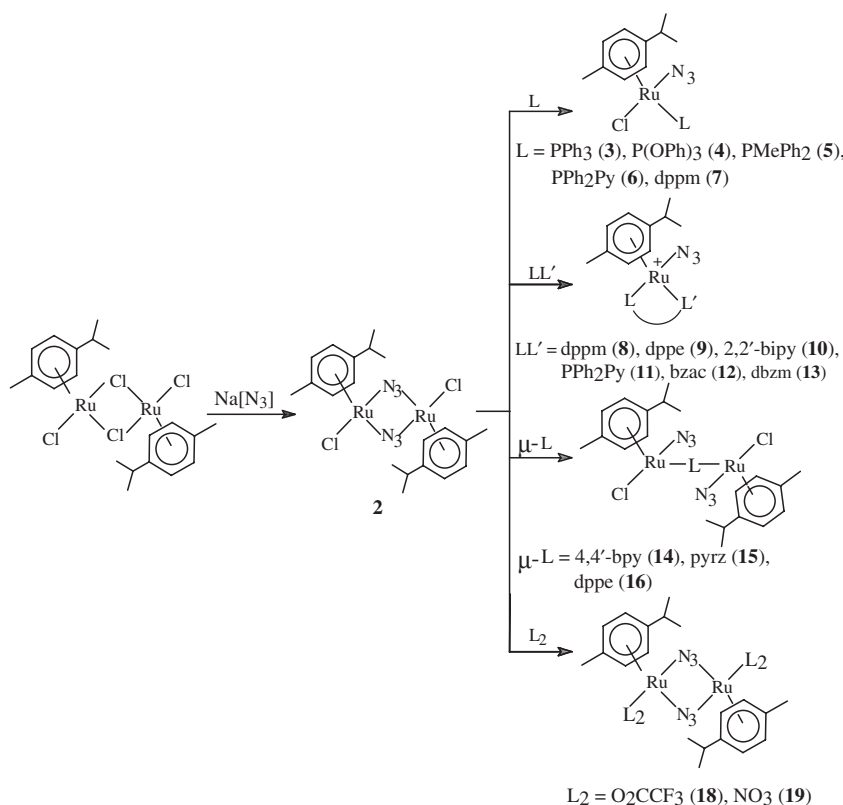
One point worth mentioning is that the complete metathetical reaction to obtain $[(\eta^6\text{-}p\text{-cymene})\text{Ru}(\mu\text{-N}_3)(\text{N}_3)]_2$ could not be achieved, even with prolonged reaction time, use of large excess of the ligand, use of halide scavengers or even elevated temperature; however, we reported earlier the facile synthesis and X-ray structure of $[(\eta^6\text{-C}_6\text{Me}_6)\text{Ru}(\mu\text{-N}_3)(\text{N}_3)]_2$ [5(b)]. This difference in reactivity may be solely due to the electron-rich nature of the hexamethylbenzene as compared to the *p*-cymene ligand.

Azide bridge cleavage reactions were investigated with the intention of generating a new family of azido-ruthenium complexes and the overall reactions of **2** with various ligands is depicted in scheme 1.

2.1. Monodentate phosphine complexes, $[(\eta^6\text{-}p\text{-cymene})\text{Ru}(\text{N}_3)\text{Cl}(\text{L})]$

The reaction of $[(\eta^6\text{-}p\text{-cymene})\text{Ru}(\mu\text{-N}_3)\text{Cl}]_2$ (**2**) with two equivalents of tertiary phosphines, **L**, namely PPh_3 , PMe_2Ph , $\text{P}(\text{OPh})_3$, PPh_2Py and dppm {bis(diphenylphosphino)methane, $\text{Ph}_2\text{PCH}_2\text{PPh}_2$ } in acetone at room temperature cleanly cleaved the azide bridge to afford monomeric neutral complexes, $[(\eta^6\text{-}p\text{-cymene})\text{RuCl}(\text{N}_3)(\text{PPh}_3)]$ (**3**), $[(\eta^6\text{-}p\text{-cymene})\text{RuCl}(\text{N}_3)(\text{P}(\text{OPh})_3)]$ (**4**), $[(\eta^6\text{-}p\text{-cymene})\text{RuCl}(\text{N}_3)(\text{PMe}_2\text{Ph})]$ (**5**), $[(\eta^6\text{-}p\text{-cymene})\text{RuCl}(\text{N}_3)(\kappa^1\text{-P-PPh}_2\text{Py})]$ (**6**), and $[(\eta^6\text{-}p\text{-cymene})\text{RuCl}(\text{N}_3)(\text{dppm})]$ (**7**) (scheme 1). All these complexes precipitated within few minutes of stirring. The IR spectra of these complexes clearly indicate the presence of terminally bound azido ligand in the range $2030\text{--}2044\text{ cm}^{-1}$, comparable to those found in closely related isoelectronic complexes $[\text{Cp}^*\text{RhCl}(\text{N}_3)\text{L}]$ ($\text{Cp}^* = \eta^5\text{-C}_5\text{Me}_5$; $\text{L} = \text{PR}_3$) [8]. The peak positions and integration of ^1H NMR spectra are consistent with the proposed structures and showed the enantiomeric nature of these complexes due to the chiral metal center. In all cases, the protons from *p*-cymene showed overlapping peaks at their usual respective positions. The $^{31}\text{P}\{^1\text{H}\}$ NMR spectra of these complexes are also consistent with the proposed structures.

Surprisingly, reaction of **2** with AsPh_3 and SbPh_3 under similar reaction conditions fails to cleave the azide bridges as evident from the unchanged stretching frequency



Scheme 1. Schematic diagram of the work described in this article.

of ν_{N_3} in the IR spectra when compared with **2** (2057 cm^{-1}). Our earlier work on the hexamethylbenzene analog readily afforded $[(\eta^6\text{-C}_6\text{Me}_6)\text{RuCl}(\text{N}_3)(\text{MPh}_3)]$ ($\text{M} = \text{As}, \text{Sb}$) [5a].

In an attempt to elucidate the detailed structure, X-ray analysis of $[(\eta^6\text{-}p\text{-cymene})\text{RuCl}(\text{N}_3)(\text{P}(\text{OPh})_3)]$ (**4**) was carried out. The molecule consists of a piano stool structure with the Ru coordinated to *p*-cymene, $\text{P}(\text{OPh})_3$, Cl, and azide. The ORTEP diagram of the complex is shown in figure 1 and selected bond lengths and angles are shown in table 1. There is nothing unusual from the crystallographic data except that one phenyl of $\text{P}(\text{OPh})_3$ has 80% occupancy at one place. The $\text{Ru}(1)\text{--Cl}(1)$ bond length remains more or less the same as that of the starting dimer; however, as expected, the $\text{Ru}(1)\text{--N}(1)$ bond length (2.207 \AA) is significantly longer than that of the bridging azide ($\mu\text{-}1,1$). The $\text{Ru}(1)\text{--N}(1)\text{--N}(2)$ angle of 124.5° is slightly wider than that of **2** (122.07°) but comparable to the data obtained by Bates *et al.* The angle $\text{N}1\text{--N}2\text{--N}3$ is slightly bent with an angle of $172.5(5)^\circ$.

2.2. Cationic and neutral chelate complexes, $[(\eta^6\text{-}p\text{-cymene})\text{Ru}(\text{N}_3)(\text{LL}')]^{+ / 0}$

The reaction of **2** and two equivalents of some potentially chelating ligands in the presence of NH_4BF_4 or NH_4PF_6 at reflux in methanol yielded cationic complexes $[(\eta^6\text{-}p\text{-cymene})\text{Ru}(\text{N}_3)(\text{LL}')]^+$ ($\text{LL}' = \text{dppm}$ (**8**), dppe (**9**), 2,2'-bipy (**10**), PPh_2Py (**11**) as

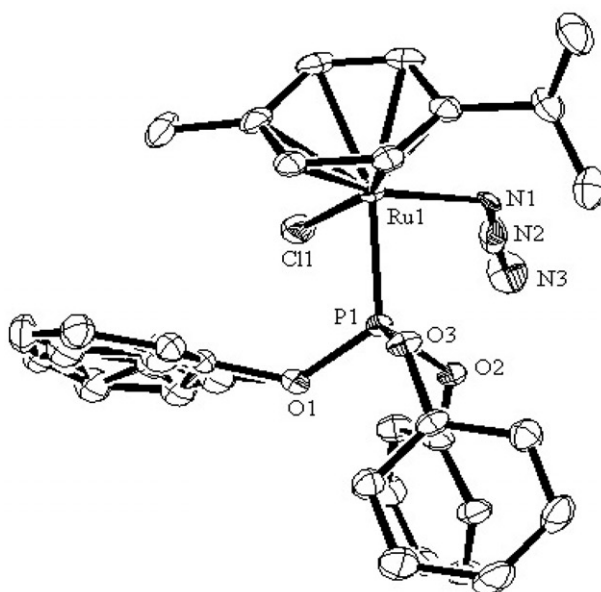


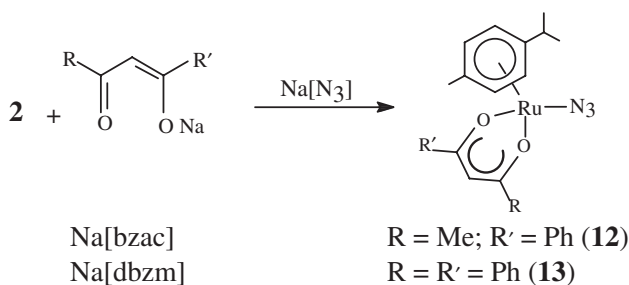
Figure 1. ORTEP of $[(\eta^6\text{-}p\text{-cymene})\text{RuCl}(\text{N}_3)\text{P}(\text{OPh})_3]$ (**4**) with all hydrogens omitted for clarity.

Table 1. Selected bond lengths and angles for $[(\eta^6\text{-}p\text{-cymene})\text{RuCl}(\text{N}_3)\text{P}(\text{OPh})_3]$ (**4**).

Bond lengths (Å)		Bond angles (°)	
Ru1–N1	2.207(4)	N1–Ru1–P1	90.14(9)
Ru1–Cl1	2.3977(12)	P1–Ru1–Cl1	86.01(4)
Ru1–P1	2.2523(10)	N1–Ru–Cl1	85.02(10)
N1–N2	1.004(6)	N2–N1–Ru1	124.5(3)
N2–N3	1.219(7)	N1–N2–N3	172.5(5)

shown in scheme 1. IR spectra of these complexes showed the stretching vibration of the terminally bound azide ligand at $ca\ 2037\text{ cm}^{-1}$. Integration of the ^1H NMR spectra of these complexes showed the presence of the chelating ligand (LL') and *p*-cymene in 1:1 molar ratio. ^{31}P NMR spectra of complexes **8** and **9** showed singlets at 27.9 and 68.07 ppm, respectively; no pendent phosphorus peaks are found from the spectra suggesting similar environments of both P atoms. The $^{31}\text{P}\{^1\text{H}\}$ NMR spectrum of **11** shows a singlet at $-10.41\ \delta$, comparable to that found in a closely related PPh_2Py chelate complex, $[(\eta^6\text{-}p\text{-cymene})\text{RuCl}(\text{PPh}_2\text{Py})]\text{BF}_4$ [9].

The reaction of **2** or the filtrate from its preparation could be used for the preparation of β -diketonate complexes as shown in scheme 2. Acetylacetonato arene ruthenium/osmium(II) complexes $[(\eta^6\text{-arene})\text{MCl}(\text{acac})]$ (M = Ru, Os) have been previously reported by Bennett *et al.* [10] starting from arene dimer with thalium salt of acetylacetonate. We have similarly found here too that the free diketones ligands did not react with **2** but with its sodium salt to give **12** or **13**.

Scheme 2. Preparation of β -diketonato azido complexes.

The neutral complexes $[(\eta^6\text{-}p\text{-cymene})\text{Ru}(\text{bzac})\text{N}_3]$ (**12**) and $[(\eta^6\text{-}p\text{-cymene})\text{Ru}(\text{dbzm})\text{N}_3]$ (**13**) were isolated in good yield, both are orange and soluble in almost all organic solvents; in particular, **12** is completely soluble in hexane. The ^1H NMR spectrum of $[(\eta^6\text{-}p\text{-cymene})\text{Ru}(\text{dbzm})\text{N}_3]$ (**13**) showed, besides the characteristic peaks corresponding to *p*-cymene ligand, 10 proton multiplets in the aromatic region and a singlet at 6.44 δ due to the phenyl groups and the γ -hydrogen of dbzm. The ^1H NMR spectrum of $[(\eta^6\text{-}p\text{-cymene})\text{Ru}(\text{bzac})\text{N}_3]$ (**12**) is similar except the γ -hydrogen of the diketonato is at 5.78 δ . Two singlets corresponding to the methyl protons appear at 2.28 δ and 2.11 δ , the latter assigned to the methyl proton of the bzac ligand while the former would belong to *p*-cymene. The IR spectra of both the complexes show bands at *ca* 1590, 1550, and 1520 cm^{-1} assignable to $\nu_{\text{C}=\text{O}} + \nu_{\text{C}=\text{C}}$ modes of the bidentate *O,O'*-donors and the band for terminally bound azide at 2037 cm^{-1} . Attempts to prepare analogous complexes from the sodium salt of dimethyl or diethyl malonate yielded intractable compound(s), which may be due to easy hydrolysis of these ligands. X-ray crystallographic determination of $[(\eta^6\text{-}p\text{-cymene})\text{Ru}(\text{bzac})\text{N}_3]$ (**12**) was carried out in order to confirm the structure in solid state, since the normal conventional spectroscopic evidences are not so conclusive to know the coordination mode of the β -diketonato ligands as they exhibit various bonding modes. In **12**, a bidentate *O,O'*-bonded "bzac" is trigonally coordinated to ruthenium while other coordination sites are occupied by almost planar *p*-cymene ring and azide ligand (figure 2). Ru1–O1 bond length of 2.0594 Å (table 2) is slightly but significantly shorter than Ru1–O2 distance of 2.0732 Å. The bond distance between ruthenium and nitrogen of azide is 2.1298 Å, significantly shorter than that found in **4**. The angle subtended by Ru1–N1–N2 is 114.75°, slightly narrower than that of **4** and the N1–N2–N3 angle is almost linear with an angle of 177.68°.

2.3. Dinuclear complexes, $[\{(\eta^6\text{-}p\text{-cymene})\text{RuClN}_3\}_2(\mu\text{-L})]$

Reaction of **2** and one equivalent of potentially bridging ligands ($\mu\text{-L}$) such as 4,4'-bipyridine (4,4'-bipy), pyrazine (pyrz), and 1,2-bis(diphenylphosphino)ethane, $\text{Ph}_2\text{PCH}_2\text{CH}_2\text{PPh}_2$ (dppe) in acetone at room temperature also cleaved the azide bridges to afford orange-red complexes $[\{(\eta^6\text{-}p\text{-cymene})\text{RuClN}_3\}_2(\mu\text{-L})]$ ($\mu\text{-L} = 4,4'\text{-bipy}$ (**14**), pyr (b) (**15**), dppe (**16**)). These compounds are soluble in chlorinated solvents, THF, acetone, acetonitrile, dmsO, and are insoluble in ether and hydrocarbons. The IR spectra of these complexes showed the terminally bound azide at 2037 cm^{-1} .

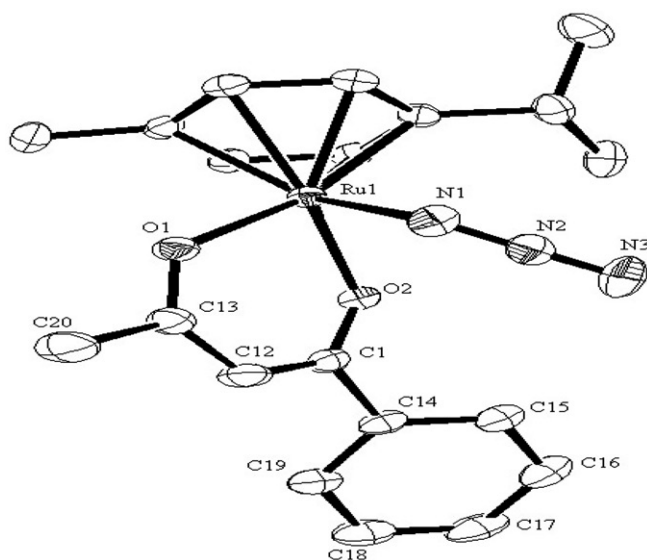


Figure 2. ORTEP of $[(\eta^6\text{-}p\text{-cymene})\text{Ru}(\text{N}_3)(\text{bzac})]$ (**12**) with all hydrogens omitted for clarity.

Table 2. Selected bond lengths and angles for $[(\eta^6\text{-}p\text{-cymene})\text{Ru}(\text{N}_3)(\text{bzac})]$ (**12**).

Bond lengths		Bond angles	
Ru1–N1	2.1298(15)	O1–Ru1–N1	83.15(5)
N1–N2	1.205(2)	O1–Ru1–N1	83.61(6)
N2–N3	1.160(2)	O1–Ru1–O2	88.75(5)
Ru1–O1	2.0594(11)	N1–N2–N3	177.68(19)
Ru1–O2	2.0732(12)	N2–N1–Ru1	114.75(12)
O1–C11	1.277(2)		
O2–C13	1.272(2)		

These complexes are also characterized with ^1H NMR and $^{31}\text{P}\{^1\text{H}\}$ NMR (for **16**). Integration of the ^1H NMR spectra of these complexes suggests one bridging ligand per two *p*-cymene ligands conforming with the suggested formulation, $[\{(\eta^6\text{-}p\text{-cymene})\text{RuClN}_3\}_2(\mu\text{-L})]$. The structure of **16** was confirmed by a single crystal X-ray diffraction study; crystals of $[\{(\eta^6\text{-}p\text{-cymene})\text{RuClN}_3\}_2(\mu\text{-4,4'}$ -bipy)] (**14**) showed only low-resolution diffraction and hence could not be solved. ^1H NMR spectrum of crude $[\{(\eta^6\text{-}p\text{-cymene})\text{RuClN}_3\}_2(\mu\text{-pyrz})]$ (**15**) revealed that the compound is contaminated with a small amount of mononuclear complex, $[(\eta^6\text{-}p\text{-cymene})\text{RuClN}_3(\text{pyrz})]$, as indicated by the appearance of two sets of doublets associated with nonbridging pyrazine at 9.09 and 8.89 ppm with one-fifth the intensity of the actual bridging pyrazine resonance at 8.60 ppm. These peaks together with associated *p*-cymene resonances disappeared on subsequent crystallizations.

Single crystals of **16**, suitable for X-ray analysis were grown from slow diffusion of hexane into concentrated solution of the compound in dichloromethane. The ORTEP diagram is shown in figure 3. Selected bond lengths and angles are shown

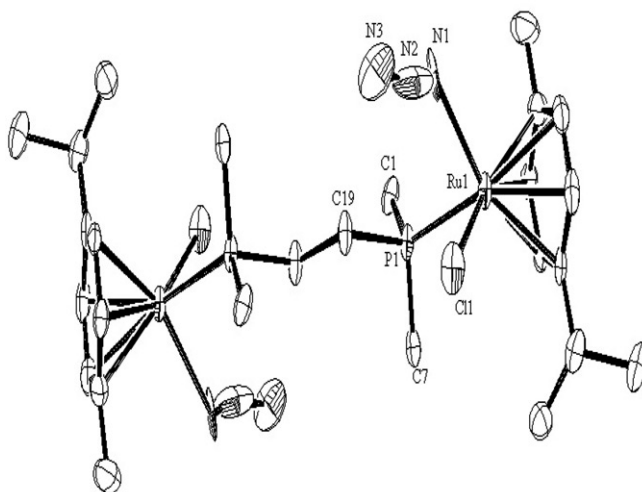


Figure 3. ORTEP of $[(\eta^6\text{-}p\text{-cymene})\text{RuN}_3\text{Cl}]_2(\mu\text{-dppe})$ (**16**) with all hydrogens and the phenyl group except the *ipso*-carbon of dppe omitted for clarity.

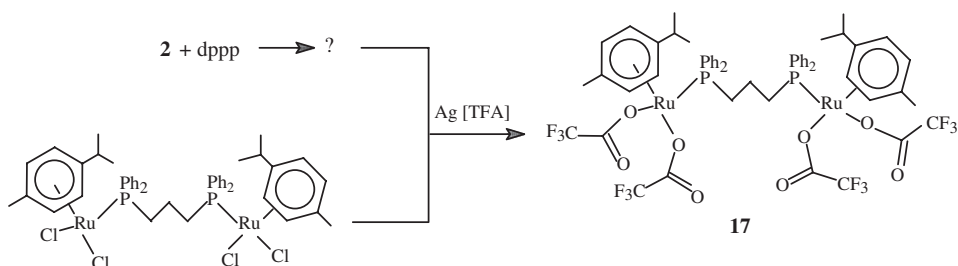
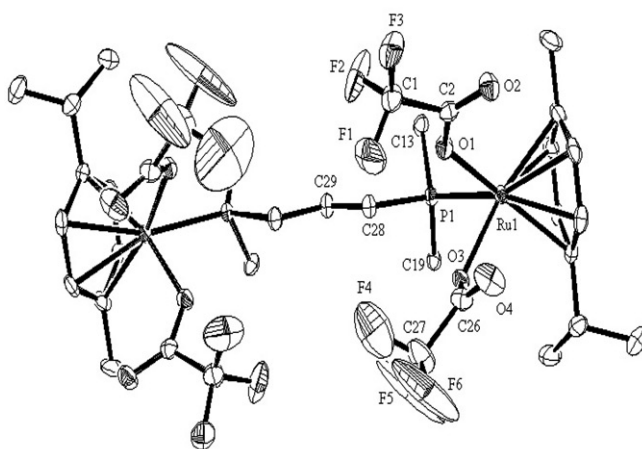
Table 3. Selected bond lengths and angles for $[(\eta^6\text{-}p\text{-cymene})\text{RuN}_3\text{Cl}]_2(\mu\text{-dppe})$ (**16**).

Bond lengths (Å)		Bond angles (°)	
Ru1–N1	2.30(5)	N1–Ru1–P1	86.66(10)
Ru1–Cl1	2.4337(17)	P1–Ru1–Cl1	84.54(5)
Ru1–P1	2.3515(13)	N1–Ru1–Cl1	91.85(13)
N1–N2	1.049(8)	N2–N1–Ru1	112.2(6)
N2–N3	1.253(9)	N1–N2–N3	165.6(9)

in table 3. The bond distances for Ru(1)–N(1) [2.304 Å] and Ru(1)–Cl(1) [2.4337(17) Å] are significantly longer than those found in $[(\eta^6\text{-}p\text{-cymene})\text{RuCl}(\text{N}_3)\text{P}(\text{OPh})_3]$ (**4**), while the bond angles N(1)–Ru(1)–Cl(1) [91.85(13)°] and N(1)–Ru(1)–P(1) [86.66(10)°], P(1)–Ru(1)–Cl(1) [84.54(5)°] reveals distortion from the actual octahedral arrangement; these angles are quite similar to those of **4**. The Ru...Ru distance is 8.412 Å.

Reaction between **2** and one equivalent or excess dpmm under similar reaction conditions unexpectedly gives only cationic chelate **8** or “dangling” P-bound dpmm complex **7**. We speculate that failure to form the expected complex $[(\eta^6\text{-}p\text{-cymene})\text{RuN}_3\text{Cl}]_2(\mu\text{-dpmm})$ may be due to the steric factor imposed by the short distance between the two phosphorous atoms.

Spectroscopic characterization of the red material isolated from reaction between **2** and dppp {1,3-bis(diphenylphosphino)propane} proved to be very difficult owing to the difficulties in separation and purification of the product(s). IR spectra of this compound(s) showed a very strong single peak at 2038 cm^{-1} assignable to terminally bound azido, suggesting the possible formation of $[(\eta^6\text{-}p\text{-cymene})\text{RuN}_3\text{Cl}]_2(\mu\text{-dppp})$ or less likely $[(\eta^6\text{-}p\text{-cymene})\text{Ru}(\kappa^2\text{-dppp})\text{N}_3]^+$, or a mixture of these two compounds. ^1H NMR and ^{31}P NMR showed overlapping signals that are too complicated for

Scheme 3. Preparation of complex **17**.Figure 4. ORTEP of $[(\eta^6\text{-}p\text{-cymene})\text{Ru}(\kappa^1\text{-}O\text{-}O_2\text{CCF}_3)_2]_2(\text{dppp})$ (**17**) with all hydrogens and the phenyl group except the *ipso*-carbon of dppp omitted for clarity.

assessing the exact integration. However, the subsequent reaction of this uncharacterized crude material with $\text{Ag}[\text{TFA}]$ yielded orange-yellow compound and the IR spectrum showed strong bands at $1712(\nu_{\text{C}=\text{O}})$, $1199(\nu_{\text{C}-\text{F}})$, and $1137(\nu_{\text{C}-\text{F}})$ cm^{-1} corresponding to coordinated trifluoroacetate, but the band corresponding to azide disappeared from this IR spectrum. It is quite surprising to find the azide ligand being displaced from the coordination sphere. ^1H NMR spectrum clearly showed the presence of *p*-cymene as well as dppp. X-ray structural analysis has revealed the compound as dimeric complex with dppp ligand bridging the two ruthenium atoms, having the formula $[(\eta^6\text{-}p\text{-cymene})\text{Ru}(\kappa^1\text{-}O\text{-}O_2\text{CCF}_3)_2]_2(\mu\text{-dppp})$ (**17**). To our knowledge, this compound is the first structurally characterized arenaruthenium complex containing coordinated trifluoroacetate (scheme 3). In order to prove the reproducibility of synthetic preparation of **17**, a reaction was performed between $[(\eta^6\text{-}p\text{-cymene})\text{RuCl}_2]_2(\mu\text{-dppp})$ [**11**] and $\text{Ag}[\text{TFA}]$ was found to yield similar compound.

Suitable X-ray quality crystals of $[(\eta^6\text{-}p\text{-cymene})\text{Ru}(\kappa^1\text{-}O\text{-}O_2\text{CCF}_3)_2]_2(\mu\text{-dppp}) \cdot \text{CH}_2\text{Cl}_2$ (**17**· CH_2Cl_2 , figure 4, table 4) were obtained from slow evaporation of dichloromethane solution. The molecule consists of ruthenium(II) fragments bridged by dppp [1,3-bis(diphenylphosphino)propane] with two trifluoroacetates per ruthenium.

Table 4. Selected bond lengths and angles for $[(\eta^6\text{-}p\text{-cymene})\text{Ru}(\kappa^1\text{-}O\text{-}O_2\text{CCF}_3)_2]_2 \mu\text{-dppp}] \cdot \text{CH}_2\text{Cl}_2 \cdot (\mathbf{17} \cdot \text{CH}_2\text{Cl}_2)$.

Bond lengths (Å)		Bond angles (°)	
P1–Ru1	2.3466(9)	O3–Ru1–P1	79.15(7)
O1–Ru1	2.102(2)	O1–Ru1–P1	80.64(7)
O3–Ru1	2.105(2)	O1–Ru1–O3	81.07(9)
C26–O3	1.264(4)	C2–O1–Ru1	130.7(2)
C2–O1	1.268(4)	C26–O3–Ru1	121.1(2)
C2–O2	1.212(4)	O2–C2–O1	131.6(3)
C26–O4	1.216(5)	O4–C26–O3	130.4(4)
C26–O3	1.264(4)		
C1–C2	1.541(5)		
C26–C27	1.530(6)		

Another coordination site is occupied by almost planar *p*-cymene with mean distance of 2.204 Å between ruthenium and the carbons of the *p*-cymene. The ruthenium oxygen bond lengths O1–Ru1 [2.102(2) Å] and O3–Ru1 [2.105(2) Å] are similar and comparable to those found in other monodentate trifluoroacetate ruthenium(II) complexes such as $[\text{Ru}(\text{O}_2\text{CCF}_3)_2(\text{H}_2\text{O})(\text{Me}_2\text{SO})_3]$ [12] and $[\text{Ru}(\text{O}_2\text{CCF}_3)_2(\text{H}_2\text{O})(\text{PMe}_3)_3]$ [13]. The Ru1–P1 distance of 2.3455(9) Å is also comparable to that of Ru1–P1 distance in **16**. The distance between the two ruthenium(II) centers is 9.500 Å, highlighting that there is substantial folding of the $-(\text{CH}_2)_3-$ moiety. The bond angles O1–Ru1–O3 [81.07(9)°], O1–Ru1–P1 [80.64(7)°], and O3–Ru1–P1 [79.15(7)°] reveal slightly distorted octahedral geometry.

2.4. Dinuclear azido-bridged nitrate and trifluoroacetato complexes, $[\{(\eta^6\text{-}p\text{-cymene})\text{Ru}(\mu\text{-}N_3)(L_2)\}_2]$

The filtrate from preparation of **2** or **2** itself when treated with $\text{Ag}[\text{NO}_3]$ in ethanol at ambient temperature afforded orange crystals that showed very strong absorption at 2077 cm^{-1} (*ca* 20 cm^{-1} higher than that of **2**) in the IR spectrum within the range of stretching of the bridging azido; bands at 1275 and 1003 cm^{-1} typical for monodentate nitrate (η^1 -nitrate) absorption [14] are also observed. ^1H NMR spectrum indicates the presence of *p*-cymene and no other useful information in regard to the composition of this compound. However, X-ray structure determination revealed the compound as binuclear azido-bridged $[(\eta^6\text{-}p\text{-cymene})\text{Ru}(\mu\text{-}N_3)(\kappa^1\text{-}O\text{-}ONO_2)]_2$ (**18**) formed from displacement of the terminal chloride from **2**. As far as our knowledge is concerned, this compound is the first structurally characterized arenoruthenium(II) nitrate complex, even though nitrate complexes of ruthenium(IV) $[\text{Ru}(\eta^3\text{-}C_{10}\text{H}_{16})\text{Cl}(\text{NO}_3)_n]$ ($n = 1, 2$) [15] as well as iso-electronic rhodium(III) complexes $\text{Cp}^*\text{Rh}(\eta^1\text{-NO}_3)(\eta\text{-Cl})_2$ and $\text{Cp}^*\text{Rh}(\eta^1\text{-NO}_3)(\eta^1, \mu\text{-}N_3)_2$ [16] have been reported earlier.

The analogous reaction with silver trifluoroacetate resulted in similar reactivity with the product showing very strong peaks at 2070 and 1686 cm^{-1} assignable to bridging azido group and $\nu_{\text{C=O}}$ of O_2CCF_3 [17], respectively. In this case also, X-ray structural analysis reveal that the product is $[(\eta^6\text{-}p\text{-cymene})\text{Ru}(\mu\text{-}N_3)(\kappa^1\text{-}O\text{-}OCOCF_3)]_2$ (**19**). It is quite apparent in these two cases that Ag^+ is the chloride scavenger.

The ORTEP diagrams of **18** and **19** are shown in figures 5 and 6, respectively, while selected bond lengths and angles are shown in tables 5 and 6, respectively. In both

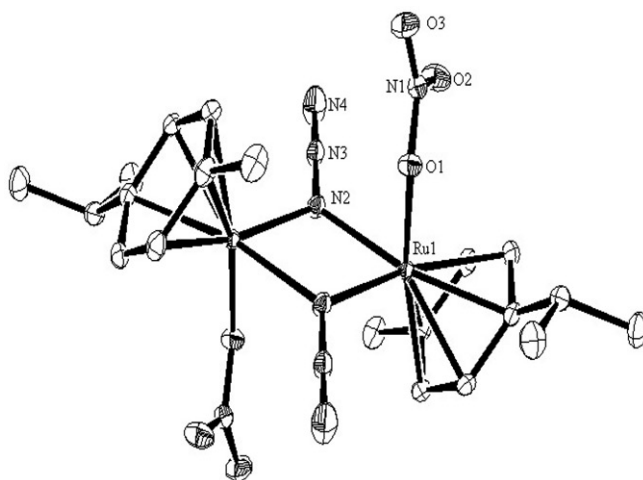


Figure 5. ORTEP of $[(\eta^6\text{-}p\text{-cymene})\text{Ru}(\mu\text{-N}_3)_2(\kappa^1\text{-O-ONO}_2)_2]$ (**18**) with all hydrogens omitted for clarity.

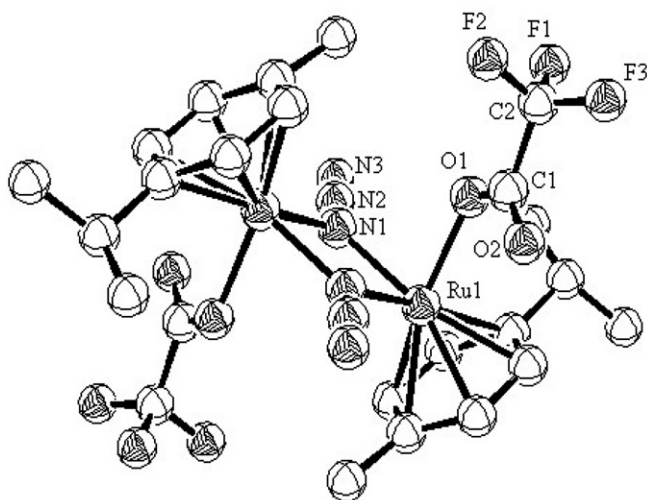


Figure 6. ORTEP of $[(\eta^6\text{-}p\text{-cymene})\text{Ru}(\mu\text{-N}_3)(\kappa^1\text{-O-OCOCF}_3)_2]$ (**19**) with all hydrogens omitted for clarity.

complexes, ligating nitrogens of azide are coordinated in planar fashion with the angles about nitrogens summing to 357.7° (for complex **18**) and 363.8° (for complex **19**); ruthenium and ligating nitrogens lie in a plane. In both complexes, the two *p*-cymene ligands are *trans* to each other and staggered. In $[(\eta^6\text{-}p\text{-cymene})\text{Ru}(\mu\text{-N}_3)(\kappa^1\text{-O-ONO}_2)_2]$ (**18**) the distance between the ruthenium and the *O*-bonded monodentate nitrate is $2.1196(14)$ Å. Similarly for **19**, the distance between the ruthenium atom and ligating oxygen atom of trifluoroacetato is $2.1024(16)$ Å, similar to that found in **17**. The distances between rutheniums and N(1) or N1#1 in both these complexes are almost the same, but longer than those found in **2**. The end-on bound azido ligands are

Table 5. Selected bond lengths and angles for $[(\eta^6$ -*p*-cymene)Ru(μ -N₃)₂(κ^1 -O-ONO₂)₂] (18).

Bond lengths (Å)		Bond angles (°)	
Ru1–N2	2.1210(15)	O1–Ru1–N2	83.27(6)
Ru1–O1	2.1196(14)	Ru1#–N2–Ru1	105.92(6)
N1–O1	1.303(2)	N2#–Ru1–N2	74.08(7)
N1–O2	1.234(2)	N2#–Ru1–O1	79.20(6)
N1–O3	1.229(2)	N1–N2–N3	178.9(2)
O3–N1–O1	116.67(16)	N3–N2–Ru1#	125.88(12)
O3–N1–O2	123.33(16)	O2–N1–O2	120.00(15)

Table 6. Selected bond lengths and angles for $[(\eta^6$ -*p*-cymene)Ru(μ -N₃)(κ^1 -O-OCOCF₃)₂] (19).

Bond lengths (Å)		Bond angles (°)	
Ru1–O1	2.1064(16)	O1–Ru1–N1	81.66(7)
Ru–N1#1	2.1169(19)	O1–Ru1–N1#1	84.61(15)
Ru1–N1	2.1144(17)	N1–Ru1–Ru1#1	128.65(15)
N3–N2	1.133(3)	Ru1–N1–Ru1#1	106.40(8)
N1–N2	1.211(3)	N1–N2–N3	178.2(2)
O2–C11	1.211(3)	O1–C11–O1	130.3(2)
O1–C11	1.272(3)		

essentially linear with bond angles of 178.9(2)° (for **18**) and 178.2(2)° (for **19**). The two ruthenium centers are separated by 3.378 and 3.388 Å for **18** and **19**, respectively.

3. Experimental

All solvents are dried and purified by the standard procedure. Reactions are performed without attempting to exclude air and all the work-up are done in air. Sodium azide, AsPh₃, PPh₃, PMe₂Ph, P(OPh)₃, dpmm, dppe, dppp, pyrazine, 2,2-bipy, 4,4'-bipy, PP₂Py, and AgNO₃ are obtained from commercial sources and used without purification. $[(\eta^6$ -*p*-cymene)RuCl₂]₂ [18] was prepared following the literature procedure. ¹H and ³¹P{¹H} NMR spectra were recorded on a Bruker 300 MHz spectrometer using Me₄Si and H₃PO₄ (85%), respectively, as internal standards. IR spectra were recorded using a Nicolet Impact Spectrophotometer. Elemental analysis was performed in Perkin-Elmer-2400 CHNS/O analyzer.

Caution: Complex **2** exploded at around 100°C while trying to determine the melting point; however, no untoward incident happened even at refluxing condition in the subsequent reactions.

3.1. Preparation of $[(\eta^6$ -*p*-cymene)RuCl(μ -N₃)]₂ (2)

Mixture of $[(\eta^6$ -*p*-cymene)RuCl₂]₂ (0.1 g, 0.163 mmol) and sodium azide (0.026 g, 0.407 mmol) was suspended in absolute alcohol (10 mL) and stirred at room

temperature; orange precipitates appeared after a few minutes and the whole suspension was stirred for 2 h to ensure that complete reaction takes place. The orange precipitates were collected by centrifuge and washed with hexane (2 × 20 mL) and vacuum dried. Additional product may be obtained by evaporating the filtrate under reduced pressure and extracting with CH₂Cl₂, filtering, and slow evaporation of this solution. Color: Orange-red, Yield: 0.085 g, 83%; C₁₀H₁₄ClN₃Ru (312.76): Calcd C 38.40, H 4.47, N 13.43; found C 38.38, H 4.42, N 13.42; IR (KBr, cm⁻¹): 2057 (s, bridging νN₃); ¹H NMR (CDCl₃, δ): 5.32 (d, J_{HH} = 6 Hz, 2H), 5.24 (d, J_{HH} = 6 Hz, 2H), 2.95 (sept, 1H), 2.27 (s, 3H), 1.29 (d, J_{HH} = 7 Hz, 6H).

3.2. Preparation of [(η⁶-*p*-cymene)RuCl(N₃)(L)] (3–7)

The mixture of [(η⁶-*p*-cymene)RuCl(μ-N₃)]₂ (0.1 g, 0.159 mmol) and **L** (0.318 mmol; 0.084 g PPh₃, 0.099 g P(OPh)₃, 0.044 g PMe₂Ph, 0.084 g PPh₂Py, 0.122 g dpmm) in acetone (15 mL) was stirred at room temperature for 3 h. After filtering the clear solution, concentrating to about 2 mL, and addition of excess diethylether or hexane, precipitate the compound as orange-red to red-brown solid. X-ray quality crystals of **4** were obtained from slow evaporation of acetone solution.

3.2.1. [(η⁶-*p*-cymene)RuCl(N₃)(PPh₃)] (3). Color: Red brown, Yield: 0.075 g, 70%; C₂₈H₂₉ClN₃PRu (575.05): Calcd C 58.48, H 5.04, N 7.30; found C 58.42, H 5.00, N 7.24; IR (KBr, cm⁻¹): 2037 (vs, νN₃); ¹H NMR (CDCl₃, δ): 7.80–7.36 (m, Ph, 15H), 5.45–4.86 (m, 4H), 2.85 (sept, 1H), 1.86–1.82 (m, 3H), 1.31–1.08 (m, 6H).

3.2.2. [(η⁶-*p*-cymene)RuCl(N₃)P(OPh)₃] (4). Color: Orange-red, Yield: 0.082 g, 82%; C₂₈H₂₉ClN₃O₃PRu (623.03): C 53.98, H 4.65, N 6.74; found C 53.95, H 4.62, N 6.78; IR (KBr, cm⁻¹): 2044 (vs, νN₃); ¹H NMR (CDCl₃, δ): 7.29 (m, Ph, 15H), 5.42, 5.35 (d, J_{HH} = 6 Hz, 2H), 5.15, 5.01 (d, J_{HH} = 6 Hz, 2H), 2.61 (sept, 1H), 1.83 (s, 3H), 1.19 (m, 6H); ³¹P{H} NMR (CDCl₃, δ): 108.4(s).

3.2.3. [(η⁶-*p*-cymene)RuCl(N₃)(PMe₂Ph)] (5). Yield: 0.064 g, 89%; C₁₈H₂₅ClN₃PRu (450.82): C 47.96, H 5.55, N 9.32; found C 47.95, H 5.52, N 9.30; IR (KBr, cm⁻¹): 2038 (vs, νN₃); ¹H NMR (CDCl₃, δ): 7.7–7.50 (m, Ph, 5H), 5.21(m, 4H), 2.55 (sept, 1H), 1.84–1.71 (m, 9H), 1.17–1.10 (m, 6H); ³¹P{H} NMR (CDCl₃, δ): 12.05(s).

3.2.4. [(η⁶-*p*-cymene)RuCl(N₃)(κ¹-*P*-PPh₂Py)] (6). Color: Orange-red, Yield: 0.080 g, 87%; C₂₇H₂₈ClN₄PRu (575.92): C 56.30, H 4.86, N 9.72; found C 56.28, H 4.82, N 9.69; IR (KBr, cm⁻¹): 2037 (vs, νN₃); ¹H NMR (CDCl₃, δ): 8.87 (d, J_{HH} = 4.5 Hz, 1H), 8.03–7.06 (m, 13H), 5.56 (d, J_{HH} = 6 Hz, 2H), 5.24 (d, J_{HH} = 6 Hz, 2H), 2.55 (sept, 1H), 1.75 (s, 3H), 1.14 (m, 6H); ³¹P{H} NMR (CDCl₃, δ): 19.16(s).

3.2.5. [(η⁶-*p*-cymene)RuCl(N₃)(dpmm)] (7). Color: Orange-red, Yield: 0.065 g, 58.6%; C₃₅H₃₆ClN₄P₂Ru (697.16): C 60.30, H 5.16, N 6.02; found C 60.24, H 5.12, N 5.08; IR (KBr, cm⁻¹): 2037 (vs, νN₃); ¹H NMR (CDCl₃, δ): 9.93–9.03 (m, 20H),

5.31–5.07 (m, 4H), 3.48–3.40 (m, 2H), 1.78 (s, 3H), 1.0, 0.78 (m, 6H); ^{31}P $\{^1\text{H}\}$ NMR (CDCl_3 , δ): 25.9 (d, P–Ru of dppm), –28.27 (dd, pendent P of dppm).

3.3. Preparation of $[(\eta^6\text{-}p\text{-cymene})\text{Ru}(\text{N}_3)(\text{LL}')^{+10} [\text{LL}' = \text{dppm} (8), \text{dppe} (9), 2,2'\text{-bipy} (10), \text{PPh}_2\text{Py} (11), \text{bzac} (12), \text{dbzm} (13)]$

A mixture of $[(\eta^6\text{-}p\text{-cymene})\text{RuCl}(\mu\text{-N}_3)]_2$ (0.1 g, 0.159 mmol), LL' (0.318 mmol; 0.122 g dppm, 0.127 g dppe, 0.05 g 2,2'-bipy, 0.084 g PPh_2Py), and NH_4PF_6 (0.400 mmol) was stirred in methanol (15 mL) at room temperature for 3 h. The solvent was removed under reduced pressure, extracted with CH_2Cl_2 and filtered to remove white insoluble material. Concentration of the filtrate and subsequent addition of excess hexane afforded red to yellow compound. X-ray quality crystals of **12** were obtained by careful layering of hexane into CH_2Cl_2 solution of the compound.

3.3.1. $[(\eta^6\text{-}p\text{-cymene})\text{Ru}(\text{N}_3)(\text{dppm})]\text{PF}_6$ (8.PF₆). Color: Orange-red, Yield: 0.078 g, 60.6%; $\text{C}_{35}\text{H}_{36}\text{N}_3\text{P}_3\text{F}_6\text{Ru}$ (806.70): C 52.11, H 4.46, N 5.21; found C 52.10, H 4.39, N 5.16; IR (KBr, cm^{-1}): 2037 (vs, ν_{N_3}), 844 (vs, $\nu_{\text{P-F}}$); ^1H NMR (CDCl_3 , δ): 9.93–9.03 (m, 20H), 5.29 (m, 2H), 5.09 (m, 2H), 3.03–2.95 (m, 2H), 2.49 (sept, 1H), 1.83 (s, 3H), 0.89 (d, $J_{\text{HH}} = 7.2$ Hz, 6H); $^{31}\text{P}\{\text{H}\}$ NMR (CDCl_3 , δ): 27.9(d), 144 (quin).

3.3.2. $[(\eta^6\text{-}p\text{-cymene})\text{Ru}(\text{N}_3)(\text{dppe})]\text{PF}_6$ (9.PF₆). Color: Orange-red, Yield: 0.080 g, 61%; $\text{C}_{36}\text{H}_{38}\text{N}_3\text{P}_3\text{F}_6\text{Ru}$ (820.74): C 52.68, H 4.63, N 5.12; found C 52.60, H 4.57, N 4.97; IR (KBr, cm^{-1}): 2037 (vs, ν_{N_3}), 844 (vs, $\nu_{\text{P-F}}$); ^1H NMR (CDCl_3 , δ): 8.48–8.32 (m, 20H), 5.17 (d, $J_{\text{HH}} = 6$ Hz, 2H), 5.02 (d, $J = 6$ Hz, 2H), 2.84 (m, 2H), 2.56 (m, 2H), 2.31 (sept, 1H), 1.75 (s, 3H), 0.84 (d, $J_{\text{HH}} = 6.9$ Hz, 6H); $^{31}\text{P}\{\text{H}\}$ NMR (CDCl_3 , δ): 68.07(s), 144.2 (quin).

3.3.3. $[(\eta^6\text{-}p\text{-cymene})\text{Ru}(\text{N}_3)(2,2'\text{-bipy})]\text{PF}_6$ (10.PF₆). Color: Yellow, Yield: 0.083 g, 90%; $\text{C}_{20}\text{H}_{22}\text{N}_5\text{PF}_6\text{Ru}$ (578.49): C 41.53, H 3.80, N 12.10; found C 41.48, H 3.74, N 12.08; IR (KBr, cm^{-1}): 2037 (vs, ν_{N_3}), 844 (vs, $\nu_{\text{P-F}}$); ^1H NMR (CDCl_3 , δ): 9.56 (d, $J_{\text{HH}} = 6$ Hz, 2H), 8.52 (d, $J_{\text{HH}} = 6$ Hz, 2H), 8.23 (t, $J_{\text{HH}} = 6$ Hz, 2H), 6.78 (t, $J_{\text{HH}} = 6$ Hz, 2H), 6.17 (d, $J_{\text{HH}} = 6$ Hz, 2H), 5.66 (d, $J_{\text{HH}} = 6$ Hz, 2H), 2.16 (s, 3H), 2.12 (sept, 1H), 1.03 (d, $J_{\text{HH}} = 6$ Hz, 6H).

3.3.4. $[(\eta^6\text{-}p\text{-cymene})\text{Ru}(\text{N}_3)(\kappa^2\text{-}P,N\text{-PPh}_2\text{Py})]\text{PF}_6$ (11.PF₆). Color: Yellow, Yield: 0.055 g, 50%; $\text{C}_{20}\text{H}_{22}\text{N}_5\text{PF}_6\text{Ru}$ (578.49): C 41.53, H 3.80, N 12.10; found C 41.49, H 3.76, N 12.04; IR (KBr, cm^{-1}): 2037 (vs, ν_{N_3}), 844 (vs, $\nu_{\text{P-F}}$); ^1H NMR (acetone- D_6 , δ): 9.24 (d, $J_{\text{HH}} = 5.5$ Hz, 1H), 9.18 (d, $J_{\text{HH}} = 5.5$ Hz, 1H), 8.44–8.30 (m, 12H), 6.21 (m, 2H), 6.09–5.86 (m, 2H), 2.59 (sept, 1H), 2.12 (s, 3H), 1.19 (m, 6H); $^{31}\text{P}\{\text{H}\}$ NMR (CDCl_3 , δ): –10.41(s).

3.3.5. $[(\eta^6\text{-}p\text{-cymene})\text{Ru}(\text{N}_3)(\text{bzac})]$ (12). Color: Orange-red, Yield: 0.062 g, 88.6%; $\text{C}_{20}\text{H}_{23}\text{N}_3\text{O}_2\text{Ru}$ (438.30): C 54.81, H 5.25, N 9.58; found C 54.76, H 5.21, N 9.53; IR (KBr): 2032 (vs, ν_{N_3}), 1589m, 1556s, 1518s ($\nu_{\text{C=O}} + \nu_{\text{C=C}}$); ^1H NMR (CDCl_3 , δ): 7.81 (d, $J_{\text{HH}} = 7.2$ Hz, 2H), 7.42–7.31 (m, 3H), 5.78 (s, 1H), 5.35 (d, $J_{\text{HH}} = 5.5$ Hz, 1H),

5.51 (d, $J_{\text{HH}} = 5.5$ Hz, 1H), 5.24 (t, $J_{\text{HH}} = 5$ Hz, 2H), 2.94 (sept, 1H), 2.28 (s, 3H), 2.11 (s, 3H), 1.36 (d, $J_{\text{HH}} = 7$ Hz, 6H).

3.3.6. $[(\eta^6\text{-}p\text{-cymene})\text{Ru}(\text{N}_3)(\text{dbzm})]$ (13). Color: Orange-red, Yield: 0.065 g, 81%; $\text{C}_{25}\text{H}_{25}\text{N}_3\text{O}_2\text{Ru}$ (500.35): C 60.01, H 4.99, N 8.40; found C 59.85, H 4.86, N 8.32; IR (KBr): 2030 (vs, ν_{N_3}), 1592m, 1543s, 1520s ($\nu_{\text{C}=\text{O}} + \nu_{\text{C}=\text{C}}$); ^1H NMR (CDCl_3 , δ): 7.83 (m, 2H), 7.38 (m, 4H), 5.79 (s, 1H), 5.48 (m, 2H), 5.20 (d, $J_{\text{HH}} = 5.5$ Hz, 2H), 2.92 (sept, 1H), 2.25 (s, 3H), 2.13 (s, 3H), 1.36 (d, $J_{\text{HH}} = 7$ Hz, 6H).

3.4. Preparation of $[(\eta^6\text{-}p\text{-cymene})\text{RuCl}(\text{N}_3)_2(\mu\text{-L})]$ [$\mu\text{-L} = 4,4'\text{-bipy}$ (14), pyrazine (15), dppe (16)]

Mixture of $[(\eta^6\text{-}p\text{-cymene})\text{RuCl}(\text{N}_3)_2]$ (0.1 g, 0.159 mmol) and L (0.159 mmol; 0.025 g 4,4'-bipy, 0.013 g pyrazine, 0.063 g dppe) in acetone (15 mL) was stirred at room temperature; **14** and **15** precipitated within 2 h as orange red solid and **16** was isolated after 3 h following the workup procedure for the preparation of **8–11**.

3.4.1. $[(\eta^6\text{-}p\text{-cymene})\text{RuCl}(\text{N}_3)_2(\mu\text{-}4,4'\text{-bipy})]$ (14). Color: Orange red, Yield: 0.080 g, 64%; $\text{C}_{15}\text{H}_{18}\text{N}_4\text{ClRu}$ (390.82): C 46.10, H 4.60, N 14.33; found C 46.02, H 4.57, N 14.28; IR (KBr, cm^{-1}): 2037 (vs, ν_{N_3}); ^1H NMR (CDCl_3 , δ): 8.84–8.74 (m, 4H), 7.61–7.50 (m, 4H), 5.47–5.19 (m, 4H), 2.95 (sept, 1H), 2.24 (s, 3H), 1.29 (m, 6H).

3.4.2. $[(\eta^6\text{-}p\text{-cymene})\text{RuCl}(\text{N}_3)_2(\mu\text{-pyrazine})]$ (15). Color: Orange red, Yield: 0.065 g, 57.5%; $\text{C}_{12}\text{H}_{16}\text{N}_4\text{ClRu}$ (390.82): C 40.85, H 4.54, N 15.87; found C 40.78, H 4.49, N 15.81; IR (KBr, cm^{-1}): 2037 (vs, ν_{N_3}); ^1H NMR (CDCl_3 , δ): 8.60 (s, 2H), 5.34–5.25 (m, 4H), 2.92 (sept, 1H), 2.26 (s, 3H), 1.33–1.28 (m, 6H).

3.4.3. $[(\eta^6\text{-}p\text{-cymene})\text{RuCl}(\text{N}_3)_2(\mu\text{-dppe})]$ (16). Color: Red, Yield: 57%; $\text{C}_{23}\text{H}_{26}\text{N}_3\text{ClPRu}$ (511.96): C 53.96, H 5.07, N 8.20; found C 53.85, H 5.01, N 8.13; IR (KBr, cm^{-1}): 2038 (vs, ν_{N_3}); ^1H NMR (CDCl_3 , δ): 7.48–7.36 (m, 20H), 5.17 (m, 8H), 2.45–2.31 (m, 6H), 1.75 (s, 6H), 1.06–0.84 (m, 6H); $^{31}\text{P}\{\text{H}\}$ NMR (CDCl_3 , δ): 26.7(d).

3.5. Preparation of $[(\eta^6\text{-}p\text{-cymene})\text{Ru}(\kappa^1\text{-O-O}_2\text{CCF}_3)_2](\mu\text{-dppp})]$ (17)

3.5.1. Method 1. The mixture of 0.06 g of the crude product isolated from reaction between **2**, dppp and $\text{Ag}[\text{TFA}]$ (0.020 g, 0.905 mmol) in ethanol (8 mL) was stirred at room temperature for 1.5 h. Solvent was rotary evaporated and the residue was extracted with CH_2Cl_2 and then filtered through short silica gel. Orange yellow X-ray quality crystals of **17**. CH_2Cl_2 were obtained on standing.

3.5.2. Method 2. Mixture of $[(\eta^6\text{-}p\text{-cymene})\text{RuCl}_2](\mu\text{-dppp})]$ (0.050 g, 0.048 mmol) and $\text{Ag}[\text{TFA}]$ (0.037 g, 0.170 mmol) in ethanol (10 mL) was stirred at room temperature for 1.5 h. Solvent was rotary evaporated and the residue was extracted with CH_2Cl_2 , filtered through short silica gel and the compound isolated after slow evaporation.

Color: Orange-yellow, Yield: 0.042 g, 61%; $C_{57}H_{54}Cl_2F_{12}O_8P_2Ru_2$ (1429.98): C 47.87, H 3.80; found C 47.80, H 3.76; IR (KBr, cm^{-1}): 1712 (vs, $\nu_{C=O}$), 1199 (vs, ν_{C-F}), 1137 (m, ν_{C-F}); 1H NMR ($CDCl_3$, δ): 7.78–7.02 (m, 20H), 5.17 (m, 8H), 2.35 (dt, 6H), 2.00 (sept, 2H), 1.98 (s, 6H), 1.42 (m, 2H), 1.06–0.84 (m, 12H); $^{31}P\{^1H\}$ NMR ($CDCl_3$, δ): 52.7(s).

3.6. Preparation of [$\{(\eta^6$ -*p*-cymene) $Ru(\mu-N_3)\}_2(L_2)$] [$L_2 = NO_3$ (18), O_2CCF_3 (19)]

3.6.1. Method 1. A mixture of **2** (0.1 g, 0.159 mmol) and $Ag[L_2]$ (0.318 mmol; $AgNO_3$, 0.054 g; AgO_2CCF_3 , 0.07 g) in ethanol (10 mL) was stirred at room temperature for 4 h. Single crystals suitable for X-ray crystallography were obtained in both cases on standing. The crystals were collected after decanting the mother liquor. Additional products were obtained by complete evaporation of ethanol under vacuum, extraction with dichloromethane, and then filtration. Subsequent concentration and addition of excess hexane afforded the compounds, which were collected and dried *in vacuo*.

3.6.2. Method 2. To the filtrate from the preparation of **2**, silver or sodium salt of the corresponding L_2 was added and the reaction mixture was stirred at room temperature for 4 h. Work up as above afforded the desired compounds.

3.6.3. [$(\eta^6$ -*p*-cymene) $Ru(\mu-N_3)((\kappa^1$ -*O*- ONO_2))_2 (18). Color: Yellow brown, Yield: 0.042 g, 78%; $C_{10}H_{14}N_4O_3Ru$ (339.32): C 35.40, H 4.13, N 16.50; found C 35.38, H 4.11, N 16.45; 1H NMR ($CDCl_3$, δ): 5.42 (d, $J_{HH} = 6$ Hz, 2H), 5.31 (d, $J_{HH} = 6$ Hz, 2H), 2.25 (sept, 1H), 2.21 (s, 3H), 0.98 (d, $J_{HH} = 7.2$ Hz, 6H); IR (KBr, cm^{-1}): 2077(vs, ν_{N_3}), 1467(s), 1387(s), 1275(s), 1003(s).

3.6.4. [$(\eta^6$ -*p*-cymene) $Ru(\mu-N_3)((\kappa^1$ -*O*- $COCF_3$))_2 (19). Color: Red, Yield: 0.055 g, 89%; $C_{12}H_{14}F_3N_3O_2Ru$ (390.33): C 36.93, H 3.58, N 10.76; found C 36.89, H 3.55, N 10.85; 1H NMR ($CDCl_3$, δ): 5.59 (d, $J_{HH} = 6$ Hz, 2H), 5.55 (d, $J_{HH} = 6$ Hz, 2H), 3.05 (sept, 1H), 2.27 (s, 3H), 1.12 (d, $J_{HH} = 6$ Hz, 6H); IR (KBr, cm^{-1}): 2070 (vs, ν_{N_3}), 1868(vs), 1195(s), 1135(m).

3.7. X-ray crystallographic determination

Details about the crystals and their structure refinement parameters are listed in table 7. The X-ray intensity data were measured on a Bruker SMART APEX CCD area detector system equipped with a graphite monochromator and a Mo- $K\alpha$ fine-focus sealed tube ($\lambda = 0.71073$ Å) operated at 1600 watts power (50 kV, 32 mA). The detector was placed at a distance of 5.8 cm from the crystal. A total of 1850 frames were collected with a scan width of 0.3° in ω and the frames were integrated with the Bruker SAINT software package using a narrow-frame integration algorithm. Data were corrected for absorption effects using the multiscan technique (SADABS) [19]. The structure was solved and refined using the Bruker SHELXTL (Version 6.1) Software Package [20].

Table 7. Crystallographic data for the X-ray diffraction studies.

	4	12	16	17	18	19
Empirical formula	C ₂₈ H ₂₉ ClN ₃ O ₃ PRu	C ₂₀ H ₂₃ N ₃ O ₂ Ru	C ₂₃ H ₂₆ ClN ₃ PRu	C ₅₇ H ₅₄ C ₁₂ F ₁₂ O ₈ P ₂ Ru ₂	C ₁₀ H ₁₄ N ₄ O ₃ Ru	C ₁₇ H ₁₄ F ₃ N ₃ O ₂ Ru
Formula weight	623.03	438.30	511.96	1429.98	339.32	390.33
Temperature (K)	95(2)	95(2)	95(2)	103(2)	95(2)	95(2)
Crystal system	Monoclinic	Monoclinic	Monoclinic	Monoclinic	Monoclinic	Monoclinic
Space group	<i>P</i> ₂ / <i>c</i>	<i>C</i> ₂ / <i>c</i>	<i>P</i> ₂ / <i>n</i>	<i>C</i> ₂ / <i>c</i>	<i>P</i> ₂ / <i>n</i>	<i>C</i> ₂ / <i>c</i>
Unit cell dimensions (Å, °)						
<i>a</i>	15.953(2)	15.0771(13)	10.1497(14)	22.153(3)	8.1638(10)	17.301(4)
<i>b</i>	8.3085(11)	8.6043(8)	14.2548(19)	14.4786(17)	17.415(2)	8.5308(15)
<i>c</i>	21.034(3)	30.068(3)	15.400(2)	20.547(2)	9.3551(11)	20.430(4)
β	100.282(2)	101.954(2)	98.024(3)	112.246(2)	112.578(2)	99.859(6)
Volume (Å ³), <i>Z</i>	2743.1(6), 4	3816.0(6), 8	2206.3(5), 4	6099.8(12), 4	1228.1(3), 4	2970.6(10), 8
Calculated density (g cm ⁻³)	1.509	1.526	1.541	1.557	1.835	1.746
Reflections collected	6537	12198	14233	18995	7838	9338
Independent reflection	6048 [<i>R</i> _{int} = 0.0255]	4593 [<i>R</i> _{int} = 0.0127]	5305 [<i>R</i> _{int} = 0.0249]	7223 [<i>R</i> _{int} = 0.0283]	2926 [<i>R</i> _{int} = 0.0219]	3523 [<i>R</i> _{int} = 0.0316]
Final <i>R</i> indices [<i>I</i> > 2σ(<i>I</i>)]	<i>R</i> ₁ = 3.99, <i>wR</i> ₂ = 11.58	<i>R</i> ₁ = 2.37, <i>wR</i> ₂ = 6.14	<i>R</i> ₁ = 6.72, <i>wR</i> ₂ = 15.46	<i>R</i> ₁ = 4.75, <i>wR</i> ₂ = 12.27	<i>R</i> ₁ = 2.15, <i>wR</i> ₂ = 5.78	<i>R</i> ₁ = 2.76, <i>wR</i> ₂ = 6.55
Goodness-of-fit on <i>F</i> ²	1.099	1.075	1.190	1.028	1.063	1.746

Supplementary material

Crystallographic data for the structural analysis have been deposited at the Cambridge Crystallographic Data Centre (CCDC), CCDC No. 280581, 280582, 280583, 280584, 280585, 280586 for complexes **4**, **16**, **17**.CH₂Cl₂, **18**, **19**, and **12**, respectively. Copies of this information may be obtained free of charge from the Director, CCDC, 12 Union Road, Cambridge, CB2 1EZ, UK (Fax: +44-1223-336033; Email: deposit@ccdc.cam.ac.uk or www: <http://www.ccdc.cam.ac.uk>).

Acknowledgments

R. Lalrempuia would like to thank the Council of Scientific and Industrial Research, India, for SRF fellowship and H.P. Yennawar thanks NSF grant CHE-0131112 for X-ray facility.

References

- [1] (a) F. Joó. *Acc. Chem. Res.*, **35**, 738 (2002); (b) R. Castarlenas, C. Vovard, C. Fischweister, P.H. Dixneuf. *J. Am. Chem. Soc.*, **128**, 4079 (2006); (c) C. Bruneau, P.H. Dixneuf. *J. Chem. Soc., Chem. Commun.*, 507 (1997); (d) T.J. Geldbach, G. Laurenzy, R. Scopeletti, P.J. Dyson. *Organometallics*, **25**, 733 (2006); (e) D. Jan, L. Delaude, F. Simal, A. Demonceau, A.F. Noels. *J. Organomet. Chem.*, **64**, 606 (2000); (f) C. Thoumazet, M. Melaimi, L. Ricard, F. Mathey, P. Le Floch. *Organometallics*, **22**, 1580 (2003); (g) J.W. Faller, J. Parr. *Organometallics*, **19**, 1829 (2000); (h) D. Amoroso, D.E. Fogg. *Macromolecules*, **33**, 2815 (2000); (i) M. Watanabe, K. Murata, T. Ikariya. *J. Am. Chem. Soc.*, **125**, 7508 (2003); (j) Y. Takai, R. Kitaura, E. Nakatani, T. Onishi, H. Kurosawa. *Organometallics*, **24**, 4729 (2005).
- [2] (a) R.E. Morris, R.E. Aird, P. del S. Murdoch, H. Chen, J. Cummings, N.D. Hughes, S. Parsons, G. Boyd, D.I. Jodrell, P.J. Sadler. *J. Med. Chem.*, **44**, 3616 (2001); (b) R.E. Aird, J. Cummings, A.A. Richie, M. Muir, R.E. Morris, H. Chen, G. Boyd, P.J. Sadler, D.I. Jodrell. *Br. J. Cancer*, **86**, 1652 (2002); (c) Y.K. Yan, M. Melchart, A. Habtemarian, P.J. Sadler. *Chem. Commun.*, 4764 (2005); (d) C.S. Allardyce, P.J. Dyson, D.J. Ellis, S.L. Heath. *Chem. Commun.*, 1396 (2001); (e) H. Chen, J.A. Parkinson, S. Parsons, R.A. Coxall, R.O. Gould, P.J. Sadler. *J. Am. Chem. Soc.*, **124**, 3064 (2002).
- [3] M.A. Bennett, K. Khan, E. Wenger. In *Comprehensive Organometallic Chemistry II*, G. Wilkinson, F.G.A. Stone, E.W. Abel (Eds), Vol. 7, 2nd Edn, Elsevier, Oxford (1995).
- [4] (a) R. Lalrempuia, M.R. Kollipara. *Polyhedron*, **23**, 3155 (2003); (b) A.L. Eckermann, D. Fenske, T.B. Rauchfuss. *Inorg. Chem.*, **40**, 1495 (2001); (c) W. Weber, P. Ford. *Inorg. Chem.*, **28**, 1088 (1986).
- [5] (a) P. Govindaswamy, P.J. Carroll, Y.A. Mozharivski, M.R. Kollipara. *J. Organomet. Chem.*, **690**, 885 (2005); (b) P. Govindaswamy, H.P. Yennawar, M.R. Kollipara. *J. Organomet. Chem.*, **689**, 3108 (2004).
- [6] R.S. Bates, M.J. Begley, A.H. Wright. *Polyhedron*, **9**, 1113 (1990).
- [7] (a) Z. Dori, R.F. Ziolo. *Chem. Rev.*, **73**, 247 (1973); (b) W. Beck, W.P. Fehlhammer, P. Pöllman, E. Schuierer, K. Feldl. *Chem. Ber.*, **100**, 2325 (1967); (c) R. Mason, G.A. Rusholme, H. Engelman, K. Joos, B. Lindenberg, H.S. Smedal. *J. Chem. Soc., Chem. Commun.*, 496 (1971).
- [8] W. Rigby, P.M. Bailey, J.A. McCleverty, P.M. Maitlis. *J. Chem. Soc., Dalton Trans.*, 371 (1979).
- [9] I. Moldes, E. de la Encarnación, J. Ros, A. Alvarez-Larena, J.F. Piniella. *J. Organomet. Chem.*, **566**, 165 (1998).
- [10] (a) M.A. Bennett, T.R.B. Mitchell, M.R. Stevens, A.C. Willis. *Can. J. Chem.*, **79**, 655 (2001); (b) D. Carmona, J. Ferrer, L.A. Oro, M.C. Apreda, C. Foces-Foces, F.H. Cano, J. Elguerno, M.L. Jimeno. *J. Chem. Soc., Dalton Trans.*, 1463 (1990); (c) R.J. Michelman, G.E. Bergman, R.A. Andersen. *Organometallics*, **13**, 869 (1994).
- [11] R.A. Zelonka, M.C. Baird. *Can. J. Chem.*, **50**, 3063 (1972).
- [12] K.Z. Malik, S.D. Robinson, J.W. Steed. *Polyhedron*, **19**, 1589 (2000).
- [13] M.O. Albers, D.C. Liles, E. Singleton. *Acta Crystallogr., Sect. C*, **43**, 860 (1987).
- [14] (a) S.A. Komaei, G.A.V. Albada, I. Mutikainen, U. Turpeinen, J. Reedijk. *Eur. J. Inorg. Chem.*, 1577 (1998); (b) R. Ballesteros, B. Abarea, A. Samadi, S.-C. Juan, E. Emilio. *Polyhedron*, **18**, 3129 (1999).

- [15] J.W. Steed, D.A. Tocher. *Polyhedron*, **13**, 167 (1994).
- [16] W.S. Han, S.W. Lee. *Inorg. Chim. Acta*, **348**, 15 (2003).
- [17] K. Nakamoto. *Infrared and Raman Spectra of Inorganic and Coordination Compounds*, 4th Edn, p. 232, Wiley, New York (1986).
- [18] M.A. Bennett, T.N. Huang, T.W. Matheson, A.K. Smith. *Inorg. Synth.*, **21**, 74 (1982).
- [19] G. Sheldrick. *SHELXL-93, Program for Crystal Structure Refinement*, Institut für Anorganische Chemie der Universität, Göttingen, Germany (1993).
- [20] Bruker Analytical X-ray Systems, Madison, USA (2002).